Detection of Wet Riparian Areas using Very High Resolution Multispectral UAS Imagery Based on a Feature-based Machine Learning Algorithm

AGILE: GIScience Series, 3, 46, 2022. https://doi.org/10.5194/agile-giss-3-46-2022
Proceedings of the 25th AGILE Conference on Geographic Information Science, 2022.
Editors: E. Parseliunas, A. Mansourian, P. Partsinevelos, and J. Suziedelyte-Visockiene.
This contribution underwent peer review based on a full paper submission.

Detection of Wet Riparian Areas using Very High Resolution Multispectral UAS Imagery Based on a Feature-based Machine Learning Algorithm

Masoume Mahboubi[1], Elena Belcore[1], Emanuele Pontoglio[2], Francesca Matrone[1,3], Andrea Lingua[1]

[1] Department of Environmental Engineering (DIATI) - Politecnico di Torino, Corso Duca degli Abruzzi 24, 10129 Turin, Italy.
[2] Freelance geologist, Italy.
[3] Department of Structural, Geotechnical and Building Engineering (DISEG) - Politecnico di Torino, Corso Duca degli Abruzzi 24, 10129 Turin, Italy.

Correspondence: Masoume Mahboubi (masoume.mahboubi@studenti.polito.it)

Abstract. Unmanned Aerial System (UAS) imagery has enabled very high-resolution multispectral image acquisition. Detection of wet areas and classification of land cover based on these images using the Machine Learning (ML) algorithm named Random Forest (RF) is our main purpose in this paper. Very high-resolution UAS images have been used as inputs for a machine learner to access the capability of different spectral bands and spectral vegetation indices, elevation, and texture features in the classification of land cover and detection of the wet riparian area in the case study in two different epochs. There are many existing methods for the classification of land cover based on UAS images, but very high-resolution centimeter-level data are of main importance in this analysis. Outstanding results have been produced in both epochs considering three extremely accurate performance analysers. Additionally, in this research, the most decisive and effective features have been discovered to compromise accuracy and the number of effectual features.

Keywords. Machine learning, classification, UAS, spectral features, land cover.

1 Introduction

Classification of land cover to detect wet and moist areas is highly important for urban and environmental planning (Chaturvedi and de Vries, 2021). Furthermore, one of the crucial pillars of climate change is connected to water in different media, from lakes and rivers to soil water. Hence, detecting water in various environmental media is one of the essential steps in facing climate change (Lidberg et al., 2020). Today, the widespread use of UAS imagery has provided a variety of very high-resolution image data sources for machine learning classifiers. The efficiency and potential of machine learning classifiers have made the classification purpose more precise and efficient (Jiang et al., 2021). UASs outperform traditional approaches for data acquisition thanks to their high temporal and spatial resolution (Merlino et al., 2020; Banerjee et al., 2020). Considering their low cost, it is possible to have several flights in different epochs (Jiménez-Jiménez et al., 2021). After data acquisition, to have a 3D map of the area, Structure from Motion (SfM) approach was implemented. There are several methods for the classification of multispectral UAS data (Iglhaut et al., 2019). RF Classifier is based on the decision of several trees (Rodriguez-Galiano et al., 2012; Lowe and Kulkarni, 2015). In this study, the performance of RF classifier in classification and wet area detection, based on three different combinations of spectral bands will be assessed, and then, the classifier's improvement after adding some extra features including spectral indices, elevation, and texture features will be analysed, and the most effectual features for classification of land cover and detection of wet soil and waterbed will be discovered. Another objective of this study is to investigate the performance of datasets (number of considered features) in the classification and if adding other features, including elevation (Normalized Digital Surface Model (nDSM)), spectral (thermal data and vegetation indexes), and texture features can be of benefits for classification. There are several studies to investigate

the classification capability based on an RF classifier (Jiang, et al., 2021; Rodriguez-Galiano, et al., 2012), but focusing on the goal of wet area detection considering different combinations of very high-resolution multispectral bands and adding other features, including elevation, spectral (thermal data and vegetation indexes), and texture in two different epochs highlights the innovation of this research.

2 Methods

The first step is to produce orthophotos and DEM based on SfM from raw UAS multispectral data; for classification, only three classes are considered: Vegetation, Water, and Ground. The dataset was acquired in two temporal epochs of April and July, and processing started with the April epoch. Three different datasets consisting of RGB, Multispectral (Red-Edge (RE), Near-Infrared (NIR)), RGB plus Multispectral for classification have been used.

2.1 Study Area

For this study, data has been acquired in the Salbertrand town in northwest Italy in two different epochs of April and July. Salbertrand, as is shown in Fig. 1, is a municipality in the province of Torino with an elevation of 1039 meters and studied riparian area located in the Salbertrand.

Figure 1. Salbertrand town, study area.

2.2 Data and Software Availability

Data were acquired using a commercial solution drone DJI Phantom 4. The drone contains a RGB sensor and separate blue, green, red, RE, and NIR sensors. During the data collection, some GCPs have been surveyed to assess the accuracy of the georeferencing of the embedded GNSS dual-frequency sensor. To perform the SfM, Agisoft Metashape software has been utilised. For machine learning, python language 3.8 with the scikit-learn package has been used; furthermore, we used open-source QGIS 3.22 software to pre-process the orthophotos and prepare the data to import into python for machine learning.

2.3 Structure from Motion

SfM technique works on the fact that several images are acquired from different angles from the area and overlapped photogrammetry produces 3D structures (Iglhaut et al., 2019). On-board Global Positioning System (GPS) of the UASs allows for location data acquisition in the collection phase, and to increase the positioning accuracy, Ground Control Points (GCPs) are collected during the campaign; in this way, the result is a high accuracy Digital Elevation Model (DEM) and orthomosaic of the study area (Turner et al., 2012). The flowchart in Fig. 2 represents the main steps included in the SfM (Iglhaut et al., 2019). After adding the images of each band into the software, the automatic interior orientation of the camera has been performed, then the images are aligned. By adding GCPs, georeferencing of the aligned photos is done and alignment is repeated to be optimized based on GCPs, then, the dense cloud is produced in the software based on the interpolation technique and a mesh is produced based on the dense point cloud, then the texture data is injected from the images into the 3D model. Finally, using the tools of the software, by-products of orthophotos of five spectral bands and DEM are produced. Orthophotos will be used in the next step to perform machine learning. In Tab. 1, results of georeferencing accuracy for checkpoints in all bands are presented for the April epoch, which is considered as a measure of 3D model accuracy.

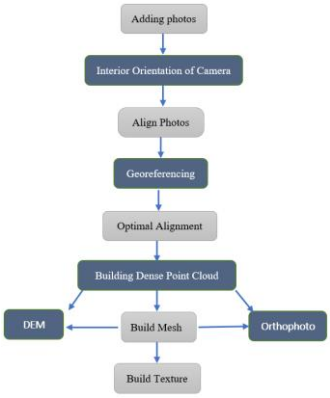

Figure 2. The procedure of SfM.

Table 1. Total error of check points in all spectral bands.

Band	Total Error (m)
Red	0.047
Green	0.056
Blue	0.048
Red-Edge	0.041
NIR	0.05

2.4 Random Forest Classifier

Random Forest classifier is based on several decision trees, in which for classification purposes, each tree decides a class, and at the end, the class with the maximum number of votes is selected as a class for the input (Maimaitijiang et al., 2020). Classification in April has been tested on three different datasets: a) combination of RGB and multispectral datasets b) RGB datasets c) Multispectral datasets including RE and NIR bands. To perform the pixel-based classification, two different portions of the study area are clipped, one for training and one for testing and validation. These spatial portions will remain constant spatially for different input datasets to have an analytical comparison at the end. The following steps have been performed for all datasets to have a final classified map and an evaluation of the accuracy of the results. Training and validation areas and their respective polygons are demonstrated in Fig. 3.

a) Data preparation for Training dataset- QGIS
b) Cross-validation- Python
c) Data preparation for Testing dataset- QGIS
d) Classification of Unseen testing dataset- Python
e) Data preparation for Validation dataset- QGIS
f) Validation- Evaluation of classification goodness- Python

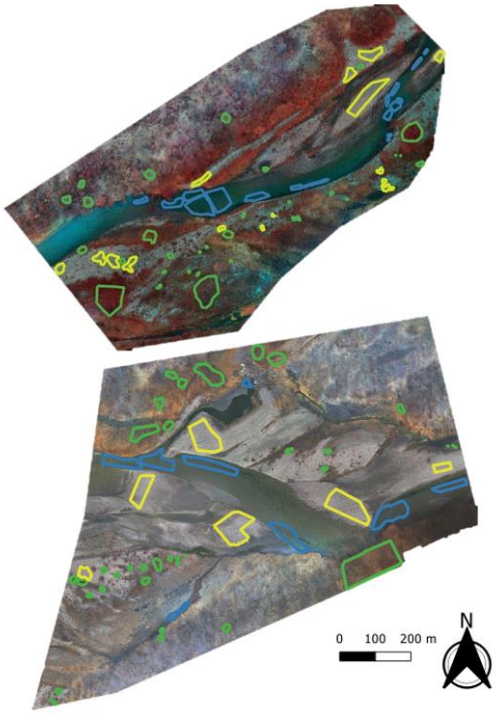

Figure 3. Top: Training area (NIR-G-R visualization) with polygons of three classes, Bottom: validation area (RGB visualization) with polygons of three classes. Blue for water, yellow for ground, green for vegetation.

The processing phase started with the April epoch. In the summer epoch, the best-selected dataset from the previous epoch beside extra features including nDSM, thermal and vegetation indexes, and texture features including Angular Second Moment, Contrast, Correlation, Variance, Inverse Difference Moment, Sum Average, Sum Variance, Sum Entropy, Entropy, Difference Variance, Difference Entropy, Information Measures of Correlation, Maximal Correlation Coefficient are added to assess the classification quality (Haralick et al., 1973) and to find out about the most effective features in the classification of the area using RF. 27 attributes for each pixel are available in this dataset. Tab. 2 shows different spectral indexes. The most essential features are selected using the "Select from Model" function in the scikit-learn package. Based on this tool, optimization is applied to the number of most effective and important features based on a median threshold.

2.5 Performance Assessment

Classification goodness is examined through evaluation tools. For this purpose, first, some concepts for accuracy assessment should be established: True Positive, True Negative, False Positive, False Negative (Williams, 2021).

- True Positive (TP): positive outcomes that the model predicted correctly.
- True Negative (TN): negative outcomes that the model predicted correctly.
- False Positive (FP): positive outcomes that the model predicted incorrectly.
- False Negative (FN): negative outcomes that the model predicted incorrectly.
- Precision: Number of correct positive results divided by the number of positive results predicted by the classifier. Eq. (1) is used to calculate the precision.

$$Precision = \frac{TP}{TP+FP} \quad (1)$$

- Recall: Number of correct positive results divided by the number of all actual samples. Eq. (2) is used to calculate the recall.

$$Recall = \frac{TP}{TP+FN} \quad (2)$$

- F1 Score: Weighted average of precision and recall and it represents how robust the classifier is. Eq. (3) is used to calculate the F1 score.

$$F1\ score = 2 * \frac{Precision*Recall}{Precision+Recall} = \frac{TP}{TP+\frac{1}{2}(FP+FN)} \quad (3)$$

Table 2. Information of different induces and author and year of introduction.

Index	Abbreviation	Formula	Author and Year
Normalised Difference Vegetation Index	NDVI	$\frac{NIR - RED}{NIR + RED}$	(Abderrazak et al., 1996)
Normalised Difference Water Index	NDWI	$\frac{Green - NIR}{Green + NIR}$	(Ceccato et al., 2002)
Normalised Difference Red-Edge	NDRE	$\frac{NIR - RE}{NIR + RE}$	(Clarke et al., 2001)
Anthocyanin Reflectance Index	ARI	$\frac{1}{Green} - \frac{1}{RE}$	(Miura et al., 2008)
Enhanced Vegetation Index 2	EVI2	$2.4 * \frac{NIR - RED}{NIR + RED + 1}$	(Miura et al., 2008)
Soil Adjusted Vegetation Index	SAVI	$\frac{NIR - RED}{(NIR + RED + L)} * (1 + L)$	(Ahamed et al., 2011)
Structure Insensitive Pigment Index	SIPI	$SIPI = \frac{NIR - Blue}{NIR - Red}$	(Xue & Su, 2017)

3 Results and Discussion

3.1 April Epoch

Based on Tab. 3, it can be recognised that RGB alone cannot produce accurate results for classification using RF but adding data from other spectral bands can improve the results. Water class is almost got detected in multispectral and combined datasets in all cases, but misclassification between ground and vegetation is still present even in the multispectral dataset. Classified areas into Vegetation and Ground have problems related to the constitution of the riverbed and the non-evergreen vegetation present in the investigated area during the cold season, besides, because of the attendance of shadow in the acquisition time in April, RF has difficulty in the classification. In Fig. 4, the results of the classification in the test area with three different datasets are visualised. Since, the best-selected dataset for this epoch is based on five spectral bands together, in the July epoch, only this dataset is used for the classification, furthermore, in the July epoch, some other features are added.

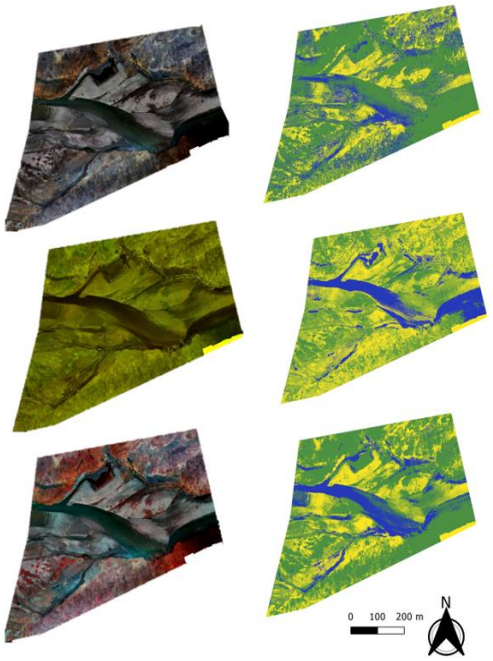

Figure 4. Left: test area in different bands (top: R-G-B true colour, middle: RE-NIR, and bottom: NIR-G-R). Right: classification results (top: with RGB, middle: with RE & NIR, bottom: with RGB and RE and NIR), blue as water, green as vegetation, yellow as ground.

Table 3. Precision, recall, and f1 score for test areas considering 3 different combinations of spectral bands.

Dataset	Classes	Precision (%)	Recall (%)	F-score (%)
RGB	Water	83	49	58
	Vegetation	57	97	72
	Ground	98	59	73
RE + NIR	Water	99	99	99
	Vegetation	65	67	66
	Ground	64	64	65
RGB+ RE + NIR	Water	99	81	89
	Vegetation	72	99	83
	Ground	99	73	84

3.2 July Epoch

In Fig. 5, the results of the classification of the test area in the July epoch with all 27 features are presented. Tab. 4, shows the results of precision, recall, and f-score of 91% on average for all classes considering 27 features.

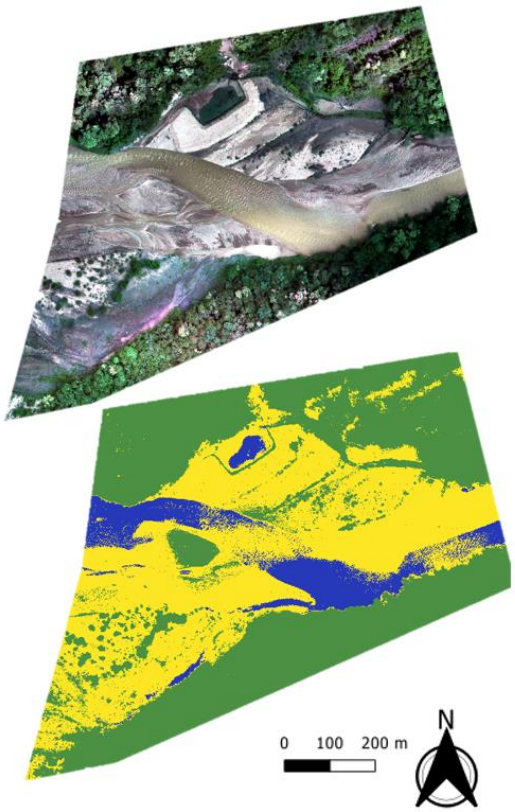

Figure 5. Top: RGB map of the test area. Bottom: classified map, blue as water, green as vegetation, yellow as ground.

3.3 Feature Selection

Fig. 6 shows the percentage of importance for each feature. As shown in Fig. 6, spectral indices including NDWI, EVI2, NDVI, SAVI, NDRE, and ARI are among the most effective features for classification, and from spectral bands, thermal and NIR and RE are the most important ones, and this is another proof that RGB dataset alone cannot achieve to the acceptable classification accuracies, even in summer epoch. Based on a median threshold, only 14 features are used to implement the classification. The result of performance analysers with all features and with only the important ones are presented in Tab. 4. It can be shown that, with only essential features, accuracy is still promising and even is increased, which represents a nice compromise between number of features and accuracy score.

Table 4. Results of performance analysis with all features vs important features.

	Precision (%)	Recall (%)	F-score (%)
27 features	91.6	91.5	91.3
14 features	93.2	92.6	92.7

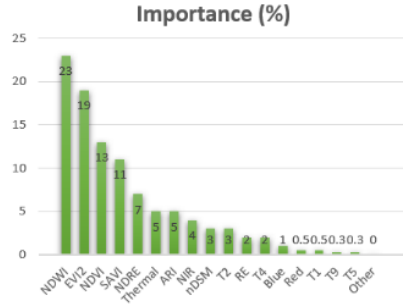

Figure 6. Importance of all features in percentage

4 Conclusion

Following our aim of identifying wet areas effectively, and the classification of two other classes, it can be emphasised that the multispectral radiometric features acquired with very high-resolution multispectral imagery associated with RF were able to do so with an excellent degree of accuracy, either in the cold season or in the summertime, with some errors mainly related to shadows due to the lack of light during the acquisition phase and constitution of the riverbed and the non-evergreen vegetation present in the area. The composition of radiometric features with additional features, including elevation, thermal, vegetation indexes, and textures features, improves the classification even more to a degree of 91% on average. Meanwhile, a compromise between the number of features and classification accuracy results in a more realistic conclusion about selected features. Based on the results, researchers can focus on the most important features in their studies, to decrease the processing time and required power alongside achieving high accuracy for the classification. In future works, other machine learning methods, such as Support Vector Machine (SVM) and deep learning methods based on convolutional neural networks, can be taken into consideration to have a comprehensive analysis of the performance of different methods for wet area detection and classification.

References

Abderrazak, B., Morin, D., Bonn, F., and Huete, A.: A review of vegetation indices, Remote Sensing Reviews. 13,95-120, https://doi.org/10.1080/02757259509532298, 1996

Agüera-Vega, F., Carvajal-Ramírez, F., Martínez-Carricondo, P., López, J. S.-H., Mesas-Carrascosa, F. J., García-Ferrer, A., and Pérez-Porras, F. J.: Reconstruction of extreme topography from UAV structure from motion photogrammetry. Measurement, 121, 127-138, https://doi.org/10.1016/j.measurement.2018.02.062, 2018.

Ahamed, T., Tian, L., Zhang, Y., and Ting, K. C.: A review of remote sensing methods for biomass feedstock production. . Biomass and Bioenergy, 35(7), 2455-2469. https://doi.org/10.1016/j.biombioe.2011.02.028, 2011.

Banerjee, B. P., Raval, S., and Cullen, P. J.: UAV-hyperspectral imaging of spectrally complex environments. International Journal of Remote Sensing, 41, 4136-4159, https://doi.org/10.1080/01431161.2020.1714771, 2020.

Ceccato, P., Gobron, N., Flasse, S., Pinty, B., and Tarantola, S.: Designing a spectral index to estimate vegetation water content from remote sensing data: Part 1: Theoretical approach,. Remote Sensing of Environment, 82, Issues 2–3,, 188-197, https://doi.org/10.1016/S0034-4257(02)00037-8, 2002.

Chaturvedi, V. and de Vries, W.: Machine Learning Algorithms for Urban Land Use Planning: A Review. Urban Sci, 5(3), 68, https://doi.org/10.3390/urbansci5030068, 2021.

Clarke, T., Moran, M., Barnes, E., Pinter, P., and Qi, J.: Planar domain indices: A method for measuring a quality of a single component in two-component pixels. . International Geoscience and Remote Sensing Symposium (IGARSS). 3. , 1279 - 1281, https://doi.org/10.1109/IGARSS.2001.976818, 2001.

Haralick, R. M., Shanmugam, K., and Dinstein, I. Textural Features for Image Classification. IEEE Transactions on Systems, Man, and Cybernetics, vol. SMC-3, no. 6, 610-621, https://doi.org/10.1109/TSMC.1973.4309314, 1973.

Iglhaut, J., Cabo, C., Puliti, S., Piermattei, L., O'Connor, J., and Rosette, J.: Structure from Motion Photogrammetry in Forestry: a Review. Remote Sensing, Curr Forestry Rep 5, 155–168, https://doi.org/10.1007/s40725-019-00094-3, 2019.

Jiang, Y., Zhang, L., Yan, M., Qi, J., Fu, T., Fan, S., and Chen, B.: High-Resolution Mangrove Forests Classification with Machine Learning Using Worldview and UAV Hyperspectral Data. Remote Sens., 13(8):1529, https://doi.org/10.3390/rs13081529, 2021

Jiménez-Jiménez, S., Ojeda-Bustamante, W., Marcial-Pablo, M., and Enciso, J.: Digital Terrain Models Generated with Low-Cost UAV Photogrammetry: Methodology and Accuracy. ISPRS Int. J. Geo-Inf.,10(5):285., https://doi.org/10.3390/ijgi10050285, 2021.

Lidberg, W., Nilsson, M., and Ågren, A.: Using machine learning to generate high-resolution wet area

maps for planning forest management: A study in a boreal forest landscape. Ambio 49, 475–486, https://doi.org/10.1007/s13280-019-01196-9, 2020.

Lowe, B. and Kulkarni, A.: Multispectral Image Analysis Using Random Forest. International Journal on Soft Computing (IJSC), 6, 1-14, https://doi.org/10.5121/ijsc.2015.6101, 2015.

Maimaitijiang, M., Sagan, V., Sidike, P., Daloye, A., Erkbol, H., and Fritschi, F.: Crop Monitoring Using Satellite/UAV Data Fusion and Machine Learning. Remote Sens., 12(9), 1357, https://doi.org/10.3390/rs12091357, 2020.

Merlino, S., Paterni, M., Berton, A., and Massetti, L.: Unmanned Aerial Vehicles for Debris Survey in Coastal Areas: Long-Term Monitoring Programme to Study Spatial and Temporal Accumulation of the Dynamics of Beached Marine Litter. Remote Sens. 12(8), 1260, https://doi.org/10.3390/rs12081260, 2020.

Miura, T., Yoshioka, H., Fujiwara, K., & Yamamoto, H.: Inter-Comparison of ASTER and MODIS Surface Reflectance and Vegetation Index Products for Synergistic Applications to Natural Resource Monitoring. Sensors (Basel),8(4), 2480-2499, https://doi.org/10.3390/s80424, 2008.

Rodriguez-Galiano, V., Ghimire, B., Rogan, J., Chica-Olmo, M., and J.P. Rigol-Sanchez.: An assessment of the effectiveness of a random forest classifier for land-cover classification. ISPRS Journal of Photogrammetry and Remote Sensing, 67, 93-104, https://doi.org/10.1016/j.isprsjprs.2011.11.002, 2012.

Tahsin, S., Medeiros, S., & Singh, A.: Assessing the Resilience of Coastal Wetlands to Extreme Hydrologic Events Using Vegetation Indices: A Review. Remote Sens., 10(9), 1390, https://doi.org/10.3390/rs10091390, 2018.

Turner, D., Lucieer, A., & Watson, C.: An Automated Technique for Generating Georectified Mosaics from Ultra-High Resolution Unmanned Aerial Vehicle (UAV) Imagery, Based on Structure from Motion (SfM) Point Clouds. Remote Sens, 4(5), 1392-1410, https://doi.org/10.3390/rs4051392, 2012.

Williams, C. K.: The Effect of Class Imbalance on Precision-Recall Curves. Neural Comput, 33 (4), 853–857, https://doi.org/10.1162/neco_a_01362, 2021.

Xue, J., & Su, B.: Significant Remote Sensing Vegetation Indices: A Review of Developments and Applications. Sensors, 1687-725X, https://doi.org/10.1155/2017/1353691, 2017.